Results and Conclusions

Equation (9) is solved by the method of successive approximations in which the slip and wall temperatures ψ_1 and ψ_s are evaluated from Eqs. (6) and (8), respectively, for each iteration. Initially, a temperature profile for $\psi(\xi)$ is assumed and used in Eq. (8) to evaluate ψ_s for a set of the parameters *Bi*, β, δ, N, and the optical depth $a_r L_c$. Subsequently, ψ_1 is obtained from Eq. (6) and used in Eq. (9) to generate a new set of values for ψ_s at every increment in ξ. Values for the slip coefficient η_1 are obtained from Ref. 6 as a function of the radiation-conduction number N. The newly obtained values for $\psi(\xi)$ are reused in Eqs. (8), (6) and (9), and the procedure is repeated until a convergence to the correct value of $\psi(\xi)$ is reached. The number of iterations for each run varied from four to seven in order to meet a tolerance of 0.5%. The results for a nonradiating medium with a prescribed wall temperature are independent of A_r when plotted as ϕ vs β and ϕ vs ξ,[2,3] where $\phi = \delta(\psi - 1) = A_r(T - T_\infty)$.

For a radiating medium, A_r and δ (or T_∞) must be specified. A representative value for $A_r = 0.02$ $\bar{K}^{-1}$ at $T_\infty = 291$ K was chosen and kept constant in the analysis. The present results are also shown in terms of ϕ in order to be consistent with the analysis of the nonradiating medium.

Table 1 shows the critical values for β_c as a function of Biot number *Bi* and the radiation-conduction number N. It can be seen that as the value of Biot number decreases, the critical value for the heat generation parameter β_c decreases. This signifies a reduction in the sample's ability to dissipate to the ambient the energy generated, preventing the sample from attaining a steady state. The effect is more severe at lower values of *Bi*. For $Bi = 100$, β_c is slightly less than the values obtained with a prescribed surface temperature ($Bi = \infty$). A reduction in *Bi* from 100 to 10 resulted in a reduction in β_c of 12.8% for the planar geometry. However, a reduction in *Bi* from 10 to 1 yielded a reduction in β_c of 60%. This percentage reduction in β_c is even far greater for lower values of *Bi*. The cylindrical and spherical geometries behaved in a similar way. The presence of radiative transfer in the analysis tends to increase the value of β_c and hence raises the tolerance of the sample to a higher limit of cyclic loading.

Figure 1 shows the centerline temperature of the sample as a function of β for the three geometries considered. Included also are the results for the case of a radiating medium with a radiation-conduction number equal to 0.3. The figure shows that the radiative effect is more significant at higher values of Biot number. This stems from the existence of a steeper temperature gradient within the sample for high values of *Bi* which in turn yields an increased value for the radiative diffusion heat flux.

References

[1]Meinkoh, D., "Heat Explosion Theory and Vibrational Heating of Polymers," *Intenational Journal of Heat Mass Transfer,* Vol. 24, 1981, pp. 645-648.

[2]Schapery, R.A., "Thermomechanical Behavior of Viscoelastic Media with Variable Properties Subjected to Cylic Loading," *Journal of Applied Mechanics,* Vol 32, 1965, pp. 611-619.

[3]Habib, I.S., "Radiation Effects on Vibrational Heating of Polymers," *Journal of Spacecraft and Rockets,* Vol. 21, Sept.-Oct. 1984, pp. 496-501.

[4]Gray, P. and Lee, P.R., "Thermal Explosion Theory," *Oxidation and Combustion Reviews,* Vol. 2, 1967, pp. 1-183.

[5]Steggerda, J.J., "Thermal Stability: An Extension of Frank-Kamenetski's Theory," *Journal of Chemical Physics,* Vol. 43, 1963, pp. 4446-4448.

[6]Siegel, R. and Howell, J.R., *Thermal Radiation Heat Transfer,* McGraw-Hill Book Co., Hemisphere Publishing Corp., 1981.

Parametric Investigations of Slender Cone Nose Bluntness Effects

L.E. Ericsson*
Lockheed Missiles & Space Company, Inc.
Sunnyvale, California

A RECENT extensive parameteric investigation of nose bluntness effects[1] provides both the incentive and the means to examine in more detail the accuracy of previously developed scaling laws for hypersonic nose bluntness effects.[2] At hypersonic speeds, the bow shock generated by a blunt nose embeds the aft body in an "entropy wake" with severely reduced dynamic pressure[3] (Fig. 1). Downstream of the nose the inviscid shear flow between the body and the bow shock can be described by a similarity profile,[3] as is indicated in Fig. 1. As a consequence, the effect of nose bluntness on the aerodynamic characteristics can be scaled using a universal scaling parameter.[2] The scaling parameter accounts for the combined effects of nose bluntness and aft body geometry (the frustum cone angle in the case of a slender cone). A check against available experimental results[4] indicated that the experimental data scatter may be larger than the error introduced by the approximations leading to the universal scaling concept.[2]

Figure 1 illustrates how the nose bluntness generates an inviscid shear flow, the entropy wake, in which the aft body geometry is embedded. The entropy wake increases with increasing nose drag, where the nose drag is determined by the drag coefficient C_{D_N} and the physical size of the nose. The figure illustrates how the same inviscid shear flow profile is generated by the three different nose geometries. The location of the flare surface in this shear flow can be shown[2] to be determined by (see Fig. 2)

$$\chi_\ell = C_{D_N}^{-1/2}(r_B/d_N)(r_B/\ell) \tag{1}$$

For a slender cone, the scaling parameter becomes[2]

$$\chi_{\ell_0} = C_{D_N}^{-1/2}(r_B/d_N)(r_B/\ell_0) \tag{2}$$

Where ℓ_0 is the length of the sharp cone, i.e.

$$r_B/\ell_0 = \tan\theta_c \tag{3}$$

For hemispherical nose bluntness, $C_{D_N} = 0.9$ and Eqs. (2) and (3) give

$$\chi_{\ell_0}^{-1} = 1.9\,\frac{d_N/d_B}{\tan\theta_c} \tag{4}$$

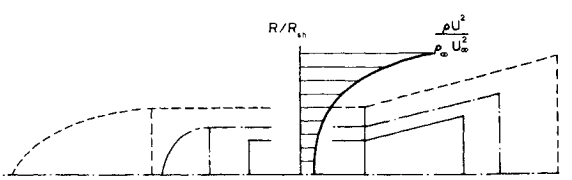

Fig. 1 Effect of nose bluntness on aft body location in "entropy wake."

Received April 6, 1984; revision received March 22, 1985.

*Senior Consulting Engineer. Fellow AIAA.

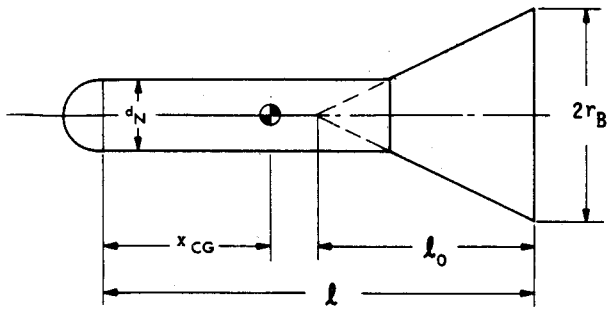

Fig. 2 Flared body geometry.

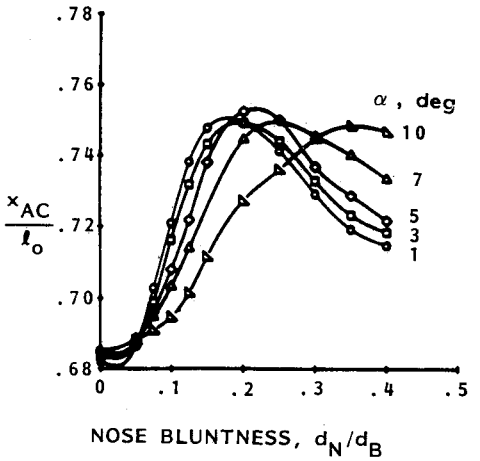

a) $M=14.3$, $\theta_c=5$ deg (Ref. 1).

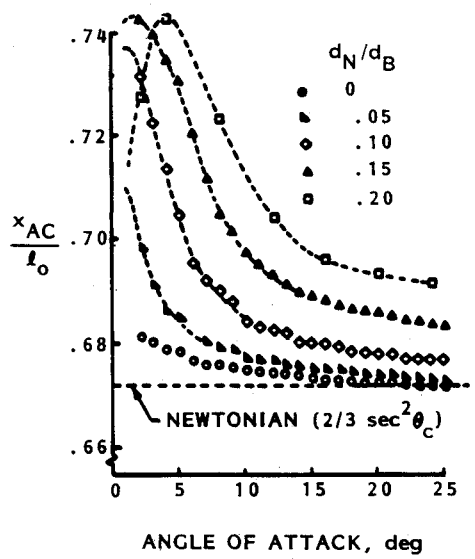

b) $M=10.14$, $\theta_c=10$ deg (Ref. 5).

Fig. 3 Effect of nose bluntness on aerodynamic center of pressure.

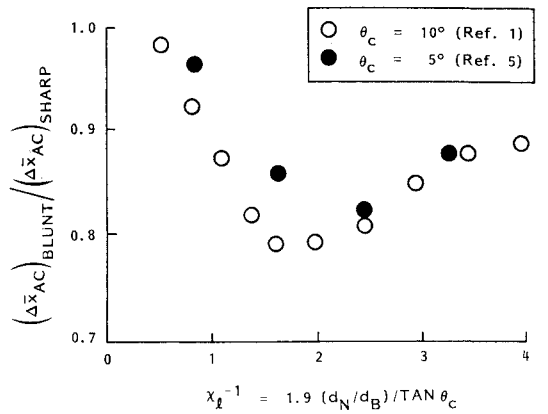

Fig. 4 Scaling of nose bluntness effects on aerodynamic center of pressure at $\alpha=0$.

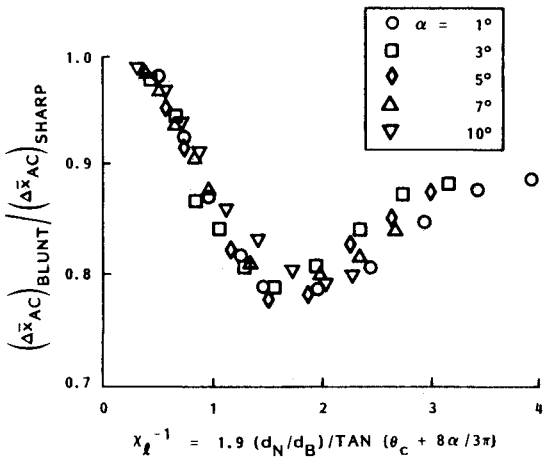

a) $M=14.3$, $\theta_c=5$ deg (Ref. 1).

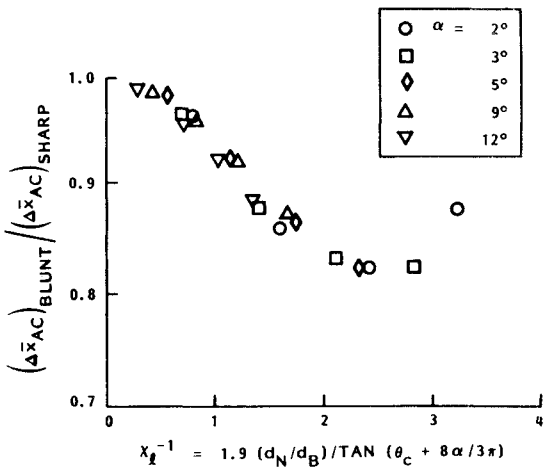

b) $M=10.14$, $\theta_c=10$ deg (Ref. 5).

Fig. 5 Scaling of nose bluntness effects on aerodynamic center of pressure at $\alpha\geq 0$.

Figure 3 shows the center of pressure determined in two recent parametric investigations.[1,5] Plotting these results against $\chi_{\ell 0}^{-1}$, with $\Delta\bar{x}/\ell_0 = 1-\bar{x}_{CP}/\ell$, seems to indicate a possible scaling difficulty (Fig. 4). An alternative explanation is that the difference is caused by differences in the test arrangements, with support interference being a likely source of error.[6] One way of checking the scaling using results from only one wind tunnel is to include the angle of attack in the scaling concept. This can be done for slender cones at moderate angles of attack by representing the windward side of the cone by a tangent cone at $\alpha=0$ that has a cone angle $(\theta_c)_{\text{eff}}$, which includes the integrated effect of α on the windward loading,[3]

$$(\theta_c)_{\text{eff}} = \theta_c + \frac{8\alpha}{3\pi} \tag{5}$$

The corresponding scaling parameter is

$$\bar{x}_{\ell_0}^{-1} = 1.9\frac{d_N/d_B}{\tan(\theta_c + 8\alpha/3\pi)} \tag{6}$$

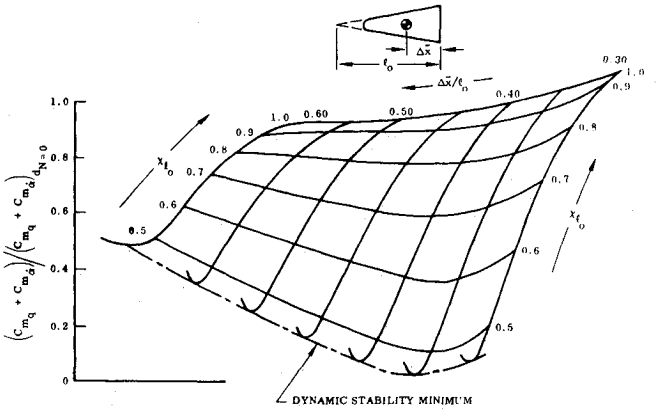

Fig. 6 Effect of oscillation center location and hypersonic similarity parameter on dynamic stability of slender blunted cones at $\alpha = 0$.

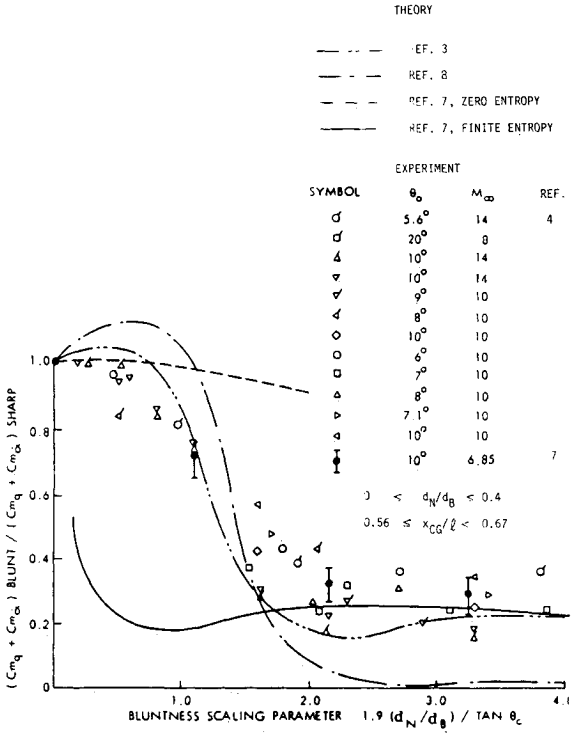

Fig. 7 Comparison between predicted and measured effects of nose bluntness on hypersonic dynamic stability of slender cones at $\alpha = 0$. (Ref. 7).

Using this effective scaling parameter the results in Figs. 3a and 3b can be represented as is shown in Figs. 5a and 5b, respectively. Comparing Figs. 4 and 5, one has to draw the conclusion that the difference between the results obtained in different tunnels is likely to be larger than the error introduced by use of the universal scaling concept. The results in Fig. 5 show further that the effects of moderate angles of attack are well represented by use of the effective scaling parameter $\bar{\chi}_{\ell_0}$ [Eq. (6)].

Computations using the embedded Newtonian theory,[3] on which the universal scaling concept[2] is based, gives the pitch damping results shown in Fig. 6. It can be seen that variations in the center of gravity within the practical range $0.33 \leq \Delta\bar{x}/\ell_0 \leq 0.44$ have little effect on the dynamic nose bluntness effect. Consequently, the universal scaling parameter can be used to compare most dynamic test results, as was done in Ref. 4 and has been done by Khalid and East[7] (see Fig. 7).

A close examination of the experimental results of parametric investigations of nose bluntness effects on the hypersonic aerodynamic characteristics of slender cones reveals that the data scatter, when comparing results from different wind tunnels, is likely to be larger than the error introduced by the approximations leading to the universal scaling concept for hypersonic nose bluntness effects described in Ref. 2.

References

[1]Bryan, M.D., Calloway, R.L., and Blackstock, T.A., "Fine-Cut Bluntness Effects on the Hypersonic Static Stability of a 10 Degree Cone," AIAA Paper 84-0503, Jan. 1984.

[2]Ericsson, L.E., "Universal Scaling Laws for Hypersonic Nose Bluntness Effects," *AIAA Journal,* Vol. 7, 1969, pp. 2222-2227.

[3]Ericsson, L.E., "Unsteady Embedded Newtonian Flow," *Astronautica Acta,* Vol. 18, Nov. 1973, pp. 309-330.

[4]Ericsson, L.E., Guenther, R.A., Stake, W.R., and Olmsted, G.S., "Combined Effects of Nose Bluntness and Cone Angle on Slender Vehicle Unsteady Aerodynamics," *AIAA Journal,* Vol. 12, May 1974.

[5]Stetson, K.F. and Lewis, A.B., "Aerodynamic Comparison of a Conical and Biconic Re-entry Vehicle," AIAA Paper 77-1161, Aug. 1977.

[6]Ericsson, L.E. and Reding, J.P., "Review of Support Interference in Dynamic Tests," *AIAA Journal,* Vol. 21, Dec. 1983, pp. 1652-1666.

[7]Kahlid, M. and East, R.A., "Stability Derivatives of Blunt Slender Cones at High Mach Numbers," *Aeronautical Quarterly,* Vol. 30, 1979, pp. 559-589.

[8]Rie, H., Linkiewicz, E.A., and Bosworth, F.D., "Hypersonic Dynamic Stability, Part III, Unsteady Flow Field Program," FDL-TDR-64-149, Jan. 1967.